

Experimental Studies of a Heat Pump with Microprocessor Control on an Animal Farm

Omarov Rashit¹, Ivaylo Stoyanov², Demessova Saule³, Murat Kunelbayev⁴ and Yerzhigitov Yerkin⁵

¹*Kazakh Scientific Research Institute of Mechanization and Electrification of Agriculture, Almaty, Republic of Kazakhstan.*

²*University of Ruse Department of Automatics & Mechatronics, Ruse. Republic of Bulgaria.*

^{3,5}*Kazakh National Agrarian University, Almaty, Republic of Kazakhstan.*

⁴*Kazakh State Women's Teacher Training University, physical-mathematical faculty, Almaty, Republic of Kazakhstan.*

Corresponding Author; Murat Kunelbayev⁴, 050000, Almaty, Republic of Kazakhstan.

Abstract

This article is devoted to experimental studies of a heat pump with microprocessor control on an animal farm. During the experiment, three versions of the heat pump were used. The compressor is better cooled when it is closer to the evaporator than when it is located centrally, this indicates a higher cooling capacity, which can be observed according to the heat energy meter shown in Fig. 8. The milk temperature during the experiment is reduced from 35 to 10°C. The best temperature mode of the condenser is provided when the compressor is located near the evaporator. It is lower by 7-8°C than in the other 2 variants. The results show that the location of the compressor affects the performance of the VT. The values of the energy conversion coefficient in two variants are from 2.5 to 4.5 units. In the third variant it is 4.5, which is 10% higher than in the 2nd and 15% than in the 1st variant.

Keywords: heat pump, compressor, evaporator, microprocessor, condenser

INTRODUCTION

In the work of BALDASSIN J.R. estimated the electric power at processing milk with the help of the heat pump. They observed daily energy consumption of 1,064 kWh for the production of 4000 liters of milk, which had the following shares: cooling (23.01%); pasteurization heating (16.1%); heating water for sanitation and cleaning (6.19%); storage in the refrigerator (7.02%); other uses as milking, aeration, volumetric reservoir (47.68%). Therefore, among all the energy spent, 30.04% was consumed in cooling and 22.28% in heating systems [1].

Modern dairy plants have partially used their thermal capacity

from the cooling system. Electrical resistors are used for heating, which increases because electric heaters consume a lot of energy compared to heat pumps [2].

The potential of heat pumps for water and spatial heating with simultaneous cooling and heating was demonstrated [3,4,5]. MA et al. suggested using a solar energy heat pump in farms, however, using either heating or cooling individually [6]. In addition, some heat pumping systems are studied for home use; but in a few studies using different energy sources [7,8,9].

Dairy plants are potential customers for heat pumps, as they can use heat from the condensation of the milk storage / cooling system, use it to heat water for cleaning and other production processes, reducing energy consumption.

Renewable sources of energy for stationary heating motors [10,11] and cooling systems [12] were investigated. Dairy farms have enough closed animal waste that can be used to produce biogas, thus being a source of renewable energy for the management of heat pumps. In the article CERVI et al. and MARTINS & OLIVEIRA have proved the possibility of using biogas while driving stationary engines for power generation, as a way to increase the sustainability of livestock production and decentralization of energy production [13,14].

The natural CO₂ fluid has been shown as a promising alternative refrigerant, especially in heating pumps due to sliding temperature heat removal into the gas cooler and performance associated with various benefits. Experimental studies of thermal applications were presented by Nexa [15] and Kim et al. [16]. Neksa et al. [17] and White et al. [18] experimentally investigated the effect of discharge pressure, water supply and temperature in a heat pump. For the food industry, the influence of the injection pressure on the operation of the CO₂ heat pump has been experimentally

investigated for the simultaneous production of refrigeration and water heating up to 90°C [19]. The effect of discharge pressure on simultaneous air conditioning and water heating has been experimentally studied [20]. Sten [21] presented the effect of water inlet temperature for a combination of spatial and water heating. Cho et al. [22] studied the performance of a CO₂ heat pump by changing the charge refrigerant in a standard cooling mode to show the importance of refrigerant flow to achieve a better performance. Kim et al. [23] conducted an experimental study of CO₂ to study the effect of the internal heat exchanger using water as a secondary fluid for both sides with underlining only when heated. Sarkar et al. [24] numerically studied the effect of water temperature at the inlet, compressor speed and heat exchanger for simultaneous water cooling and

heating. Yokoyama et al. [25] numerically studied the effect of ambient temperature on the performance of a water heating system with a CO₂ heat pump. Cabello et al. [26] experimentally investigated the influence of evaporation temperature and temperature at the gas cooler outlet on the optimal gas cooler of pressure and by means of comparisons with the available correlations. [27] developed a hybrid system for the use of renewable energy sources for local consumers in agriculture, which consists of tubular helio collectors with a capacity of 3 kW. In [28], the thermal power of a combined system with solar collectors and a heat pump.

METHODOLOGY OF THE STUDY

As it was said in the section of research methods, the analysis of the characteristics of HP is carried out for 3 options:

First option - the compressor does not cool. For this purpose, a screening cylindrical partition is installed between the compressor sidewall and the evaporator walls.

2nd option - the compressor is located in the center of the evaporator. In this case, heat exchange will occur by radiation and convection between the heated wall of the compressor and the internal cold walls of the evaporator.

The third option - the compressor is located with a shift from the center, closer to the wall of the evaporator. It is assumed that such an arrangement - the approximation of the side wall of the compressor to the wall of the evaporator will affect the heat exchange by radiation and, in general, the cooling process.

At each experiment, temperatures are recorded at the corresponding points of the HP. The layout of the temperature sensors on the elements of the prototype is shown in Figure 1.

The sensors show: 1 - the temperature of the refrigerant at the outlet of the evaporator; 2 - temperature of the refrigerant at the inlet to the evaporator; 3 - temperature of the refrigerant at the outlet of the condenser; 4 - temperature of the refrigerant at the inlet to the condenser; 5 - air temperature in the space

around the compressor; 6 - temperature of the compressor sidewall (where the motor is located); 7 - temperature of the surface of the head of the compressor; 8 - surface temperature of the tubes of the evaporator heat exchanger. Also on the diagram are the refrigerant pressure sensors installed at the inlet and outlet of the compressor.

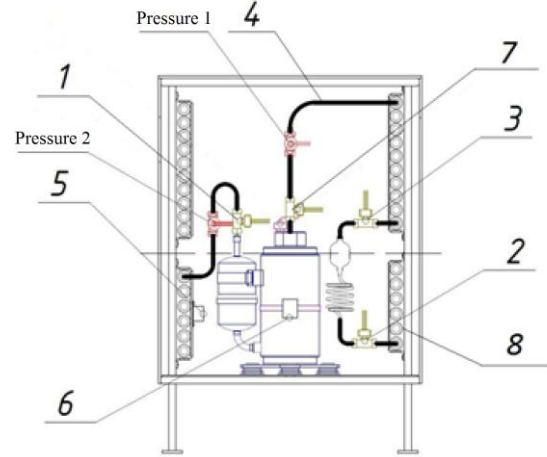
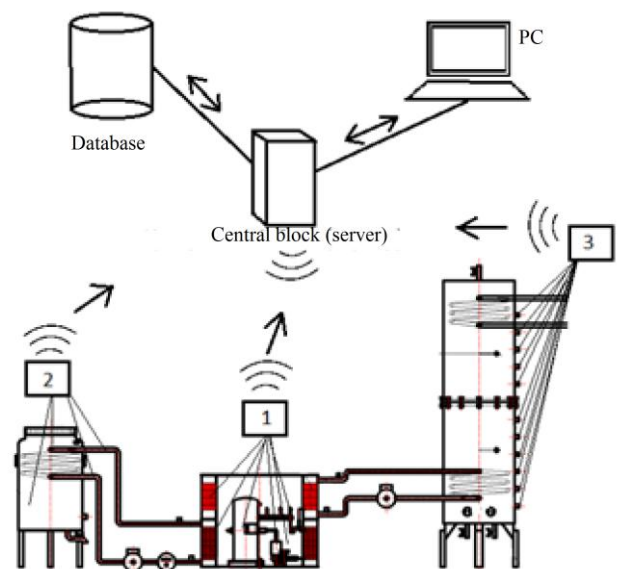


Figure 1: Sensor arrangement in the HP

Figure 1 shows the diagram of the stand and the connection of measuring instruments.



1 - heat pump module, 2 - milk cooler module, 3 - storage tank module.

Figure 2: Arrangement of the stand and connection of measuring instruments

It can be seen from the diagram that the operation of the capacitor is characterized by four sensors: 3 and 4, as well as sensors installed at the inlet and outlet of the condenser heat exchanger (Figure 3.9). They also show the temperature of the water in the storage tank.

The operation of the evaporator is characterized by four other sensors: 1 and 2, as well as sensors installed at the inlet and outlet of the evaporator heat exchanger (Figure 2). They also show the milk temperature in the milk cooler.

The temperature mode of the compressor is shown by the sensor 6 attached to the side wall, as well as the sensor 7 attached to the compressor cover. At the same time, sensor 6 indirectly characterizes the temperature state of the electric motor, which is located inside the compressor, opposite point 6. Sensor 7 characterizes the temperature under the hood where the refrigerant is directly compressed. The temperature state in the space between the compressor and the evaporator is shown by sensors 5 and 8.

The scheme of the stand schematically shows the process of collecting, transmitting, processing and storing data during research. Records of pressure and temperature indicators are conducted synchronously in time, a microcontroller with the appropriate software. The core of the information system is a central unit (server), a database, personal computers with software, as well as modules for data collection from a heat pump (1), a milk cooler (2) and a storage tank (3).

The heat pump module collects data from the following sensors from 12 temperature sensors (DS18B20 encapsulated), 2 liquid flow sensors (G1WFM) and 2 pressure sensors (Wika-R1). The milk cooler module is connected to the 4 temperature sensor (DS18B20) and one fluid flow sensor (G1WFM). The battery module collects data from 15 temperature sensors (DS18B20), arranged in series along the vertical.

The information gathering process is initiated by the central unit, sending a request to each module separately. After receiving the request, each module starts to poll the sensors and collects the data into one packet, which is then sent back to the central unit. The server, receiving packages with "raw"

data, processes them according to the appropriate algorithms for convenient storage. The server then sends the data to the database for storage. From the user's personal computer, you can view the current values using special software.



Figure 3: General view of the experimental stand

On the laboratory experimental stand (Figure 3.11), a milk cooler (right) is used as the source for the HP, and the accumulating capacity is used as a load.

Circulation of the coolant in the circuits of the milk cooler and accumulating capacity is ensured by circulating pumps.

Figure 4 shows the fragments of acquisition (a) and fabrication of HP(b and c). The main components include: TPB compressor Danfoss TX-2 R22 / 407, filter drier EK-084S, copper pipes 5 mm, microprocessors Atmel, microprocessors ARM, wireless modules Zigbee, sensors for automation, etc. The manufactured product is shown on the right a photo.

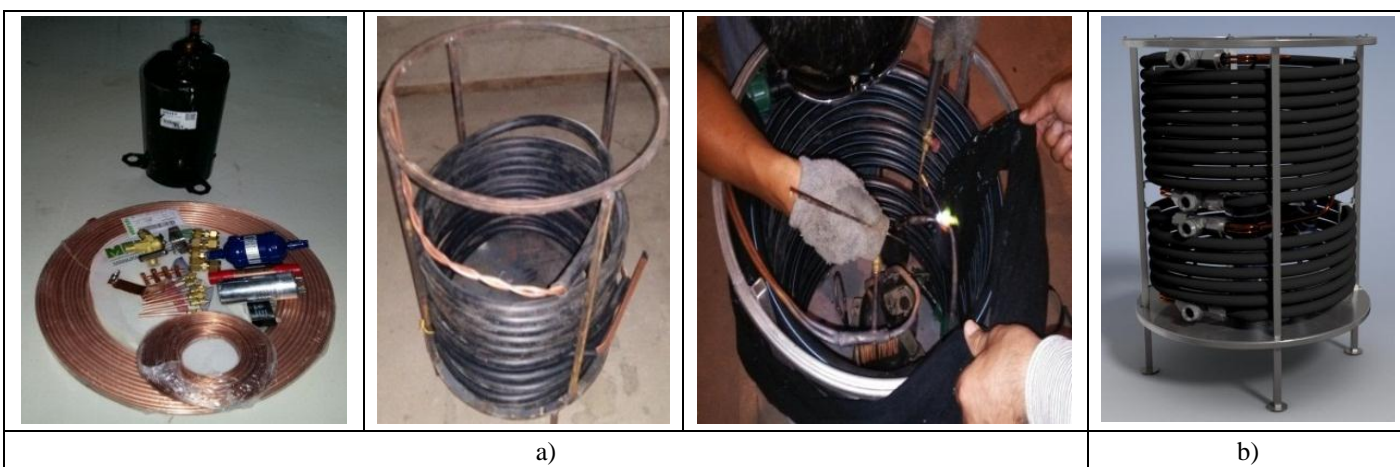
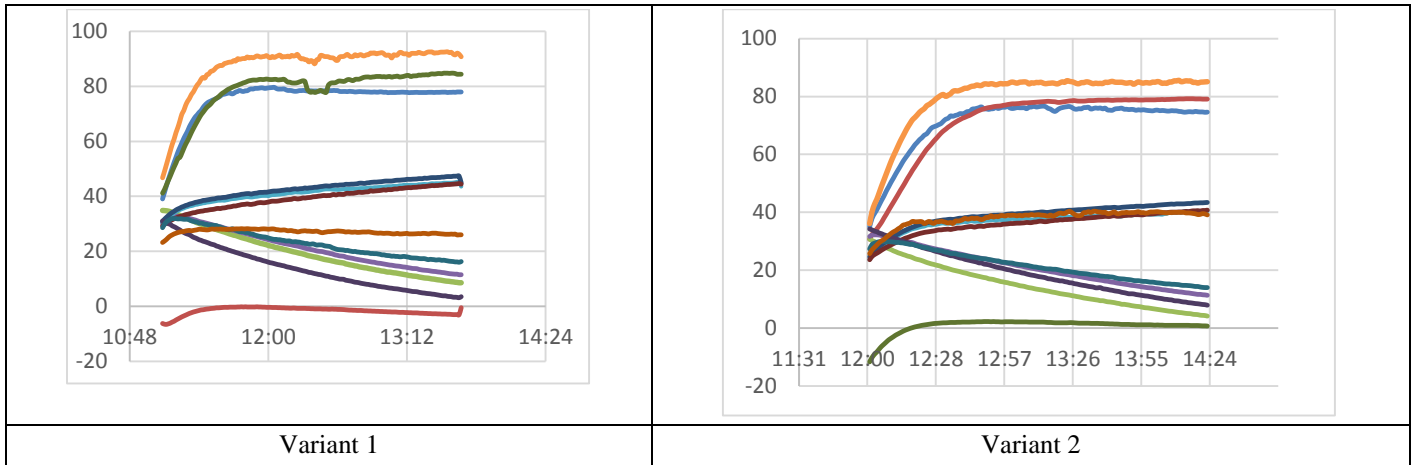


Figure 4 - a) manufacturing fragments, b) sample HP

ANALYSIS OF RESEARCH RESULTS

Graphs of temperature changes for the three compressor layouts are shown in Figures 5 a), b) and 6. The graphs show the expected values. The highest is the refrigerant temperature at the compressor outlet (sensor 4). It is the maximum (95°C) with the 1st variant, when the compressor was not cooled. The minimum (85°C) with the 3rd version, when the compressor is

close to the evaporator. The temperature difference between the input and output of the capacitor is the maximum (46°C) at the 3rd variant and the minimum (about 40°C) with the 1st variant. These figures confirm the positive effect of cooling the compressor on the internal processes of the HP. The compressor is better cooled when it is closer to the evaporator than when it is located centrally.



Variant 1 - the compressor is located at the center of the evaporator and Variant 2 - the compressor is close to the evaporator wall

Figure 5: Temperature characteristics of the heat pump

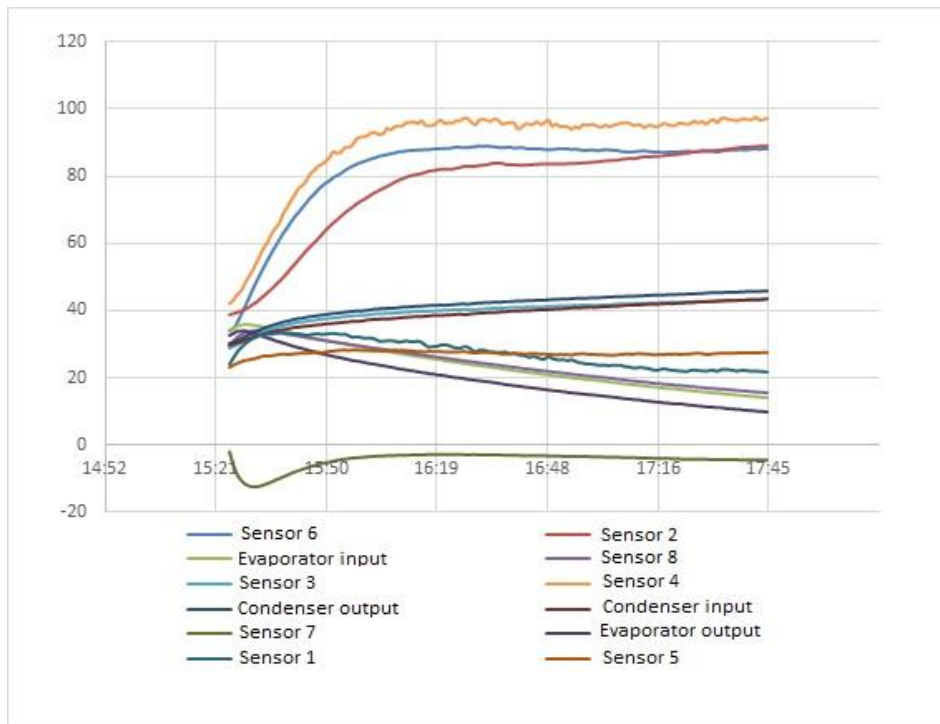


Figure 6: Temperature characteristics of the heat pump, where the compressor is shielded from the evaporator (Variant 3)

In Figure 6, the comparative temperature dependences of the condenser for 3 variants are combined. The top 3 graphs show the inlet temperatures (sensor 3), and the bottom 3 graphs at the output of the capacitor (sensor 4).

As you can see, the best temperature mode of the condenser is provided when the compressor is located near the evaporator. It is lower by 7-8°C than in the other 2 variants.

Figure 7 combines the evaporator temperature charts for the 3 options.

As can be seen, at the inlet to the evaporator (lower graphs), the refrigerant comes with a temperature of -5°C (option 1) to

-12°C (option 2). Passing through the evaporator, the temperature of the coolant rises to 28° C, in the third variant and up to 33° C in the second variant. The best temperature mode of the evaporator is provided when the compressor is located near the evaporator. It is lower by 7-8°C than in the other 2 variants.

Accordingly, this indicates a higher cooling capacity, which can be observed according to the heat energy meter shown in Figure 3.18. The milk temperature during the experiment is reduced from 35 to 10°C

Figure 8 combines the comparative temperature graphs of the compressor sidewall for 3 variants.

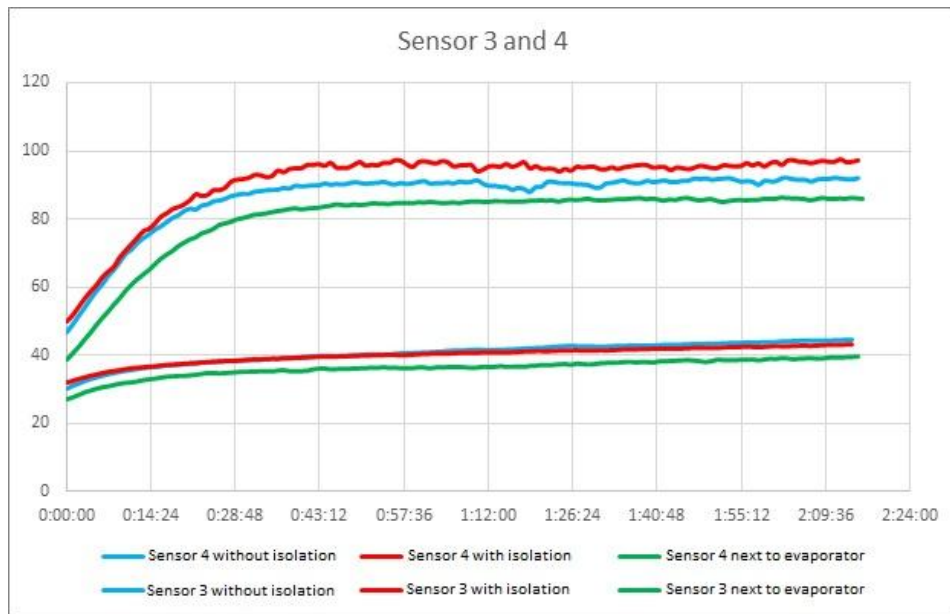


Figure 7: Charts of the refrigerant temperature at the inlet (top graphs) and the output from the condenser, with 3 variants

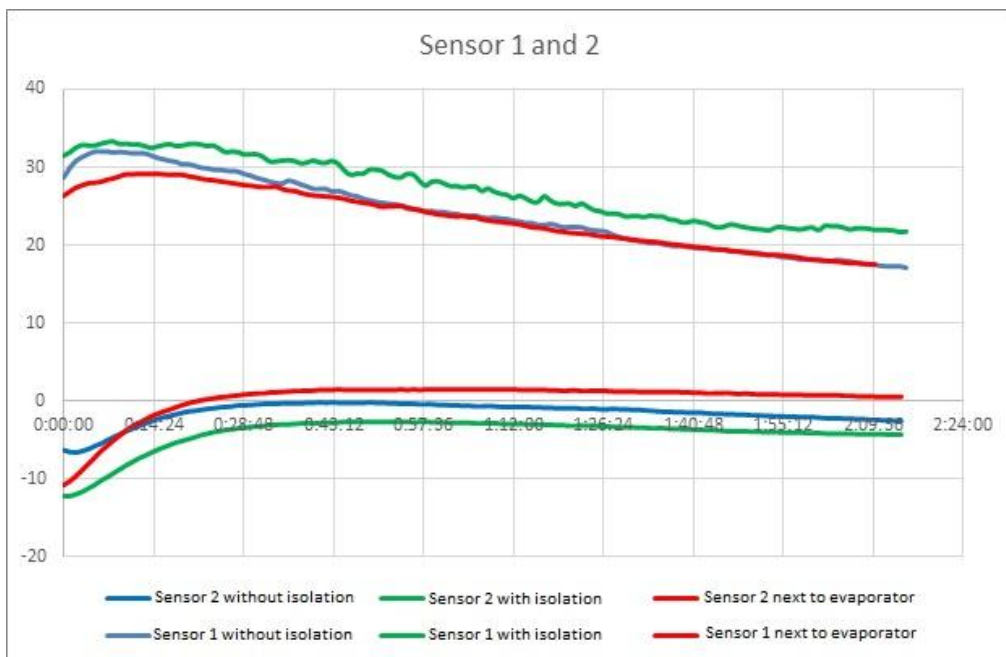


Figure 8: Graphs of inlet temperature (lower graphs) and exit from the evaporator, with 3 versions

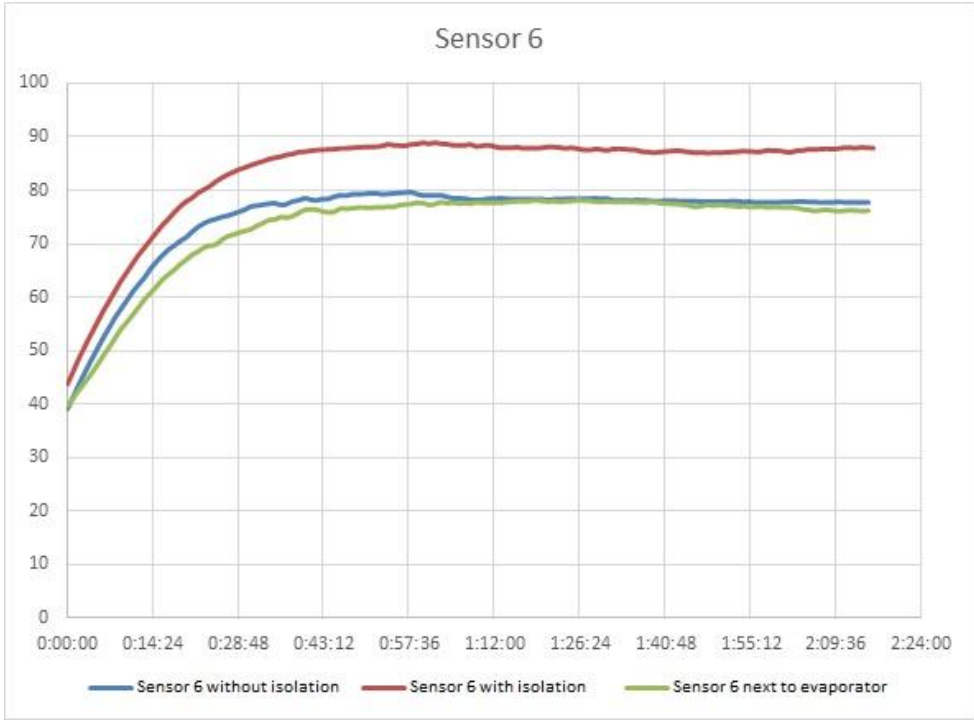


Figure 9: Compressor sidewall temperature graphs for 3 variants

The graphs show that cooling the compressor reduces its temperature. In 2 variants with cooling, it is lower by 5°C than with the 1st variant (85°C).

The distribution of air temperatures in the space between the evaporator and the compressor (sensor 5) and the surface of

the evaporator (sensor 8) are shown in Figures 5 a) and b). It is at about 20°C. When the compressor is located near the evaporator, it is lower by 10°C. This indicates a more intense absorption of heat by the evaporator. Accordingly, the compressor less heats the surrounding air.

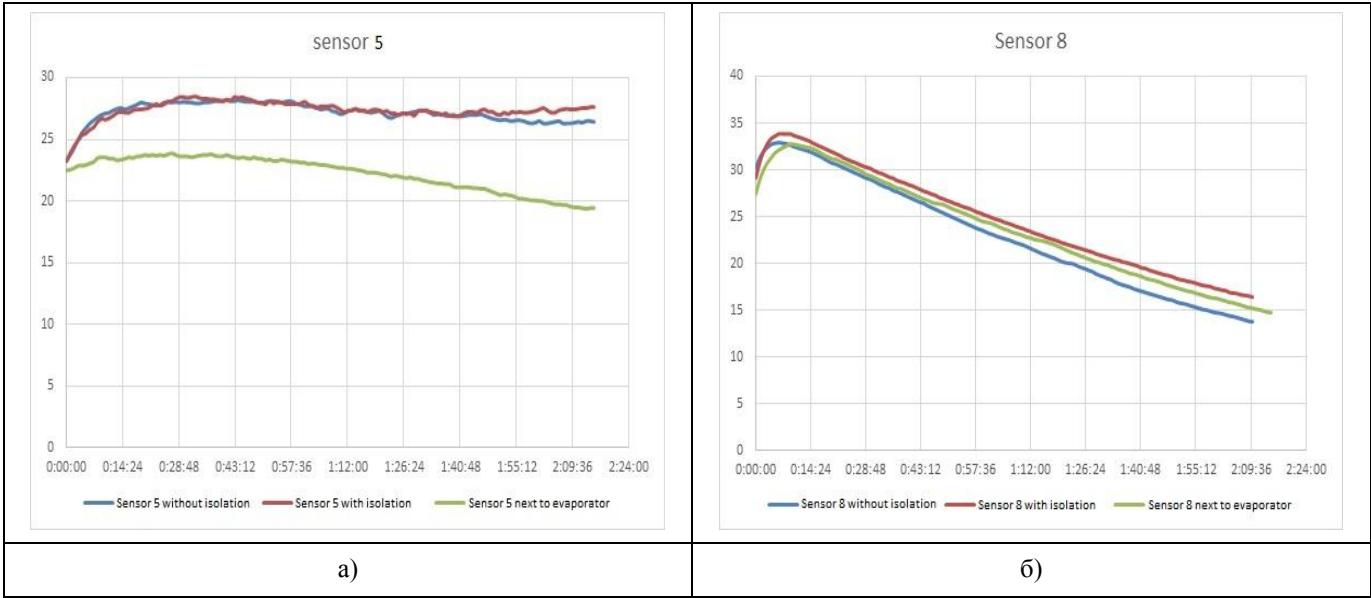


Figure 10: Graphs of air temperature in the space between the evaporator and compressor (a) and the evaporator surface temperature with 3 options

Figure 11 shows the comparative graphs of: a) the heat output and the power consumed by the compressor; and b) the cooling capacity for the tested variants.

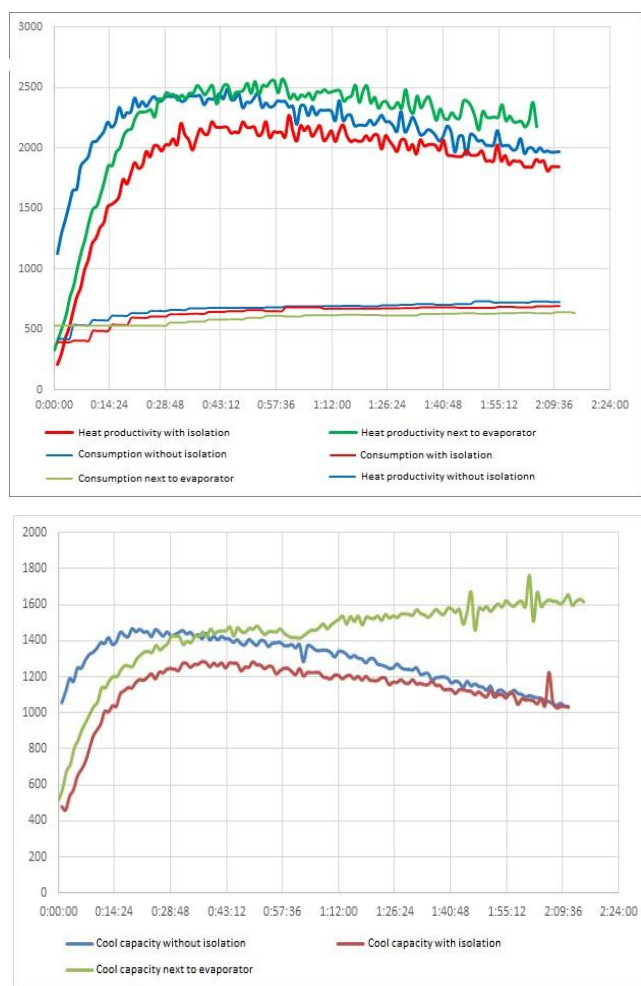


Figure 11: Heat capacity graphs (upper dependencies) and power consumption for 3 variants.

The results show that the location of the compressor affects the performance of the HP. Consumption of electricity in all cases is almost the same (the bottom three dependencies). The third option is more heat and cooling capacity. In this case, the evaporator absorbs heat generated from the surface of the compressor, which is added to the main stream. Since the temperature difference between the stack of the compressor (about 800 °C) and the evaporator (about 180 °C) is about 600 °C, we can assume that the main flux between the surfaces is radiation heat exchange. The decrease in performance in the third variant, apparently, is due to the fact that the screen between the compressor and the evaporator excludes heat exchange by radiation. At the same time, the compressor does not overheat, as its convective cooling is preserved. Charts of capacity are correlated with heat production graphs.

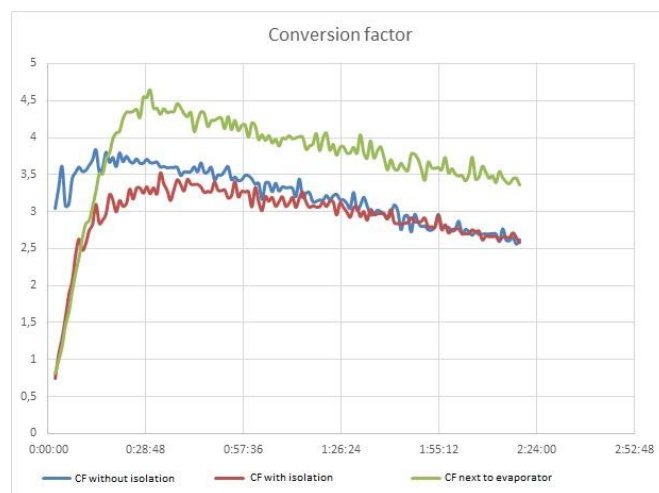


Figure 12: COP graphs for 3 variants

The cooling capacity plots of the options shown in Figure 3.26 correlate with the heat production graphs. The performance of the 1st and 3rd variants are almost the same. In the second variant it is higher. If in the 1st and 3rd variants, by the end of the process, it is about 1200 W, then in the second variant it rises to 1600 W. That is, 25% higher.

CONCLUSION

Experimental studies have confirmed the hypothesis that self-regulating cooling has been achieved, that the temperature regime of the compressor motor windings has decreased, that the heat output has increased due to an improvement in the operating mode of the compressor and the absorption of the compressor's heat. The optimum solution is found when the compressor is located with a displacement from the center and approaches the evaporator.

REFERENCE

- [1] Baldassin Jr., R. Uso racional de energia em fazendas leiteiras com bombas de calor. 2006. 176 f. Dissertação (Mestrado em Planejamento de Sistemas Energéticos) - Faculdade de Engenharia Mecânica, Universidade Estadual de Campinas, Campinas, 2006.
- [2] I Sharaf-Eldeen, Y.. Performance of heat pump water heater, HPWH systems and their impacts on electric utility loads. *Journal of Thermal Science and Engineering Applications*, New York, v. 2, p. 021008-1-021008-6, 2010.
- [3] Byrne, P.; Miriel, J.; Lenat, Y. Design and simulation of a heat pump for simultaneous heating and cooling using HFC or CO₂ as a working fluid. *International Journal of Refrigeration*, Guildford, n.32, p.1711-1723, 2009.

- [4] Pardo, N.; Montero, A.; Sala, A.; Martos, J.; Urchueguía, J. F. Efficiency improvement of a ground coupled heat pump system from energy management. *Applied Thermal Engineering*, Oxford, n.31, p.391-398, 2011.
- [5] Sebarchievici, C.; Sarbu, I. Performance of an experimental ground-coupled heat pump system for heating, cooling and domestic hot-water operation. *Renewable Energy*, Oxford, n.76, p.148-159, 2015.
- [6] Ma, K.; Jin, L.; Yan, L. Feasibility study about solar energy-air source heat pump system in cold region rural residential applications. *Applied Mechanics and Materials*, Switzerland, v.672-674, p.113-116, oct. 2014.
- [7] Stafford, A.; Lilley, D. Predicting in situ heat pump performance: An investigation into a single ground-source heat pump system in the context of 10 similar systems. *Energy and Buildings*, Lousanne, n.49, p.536-541, 2012
- [8] Luo, J.; Rohna, J.; Bayer, M.; Priess, A.; Wilkmanna, L.; Xiang, W. Heating and cooling performance analysis of a ground source heat pump system in Southern Germany. *Geothermics*, Amsterdam, n. 53, p.57-66, 2015.
- [9] Vieira, A. S.; Stewart, R. A.; Beal, C. D. Air source heat pump water heaters in residential buildings in Australia: Identification of key performance parameters. *Energy and Buildings*, Lousanne, n.91, p.148-162, 2015.
- [10] Fernandez, N.; Hwang, Y.; Radermacher, R. Comparison of CO₂ heat pump water heater performance with baseline cycle and two high COP cycles. *International Journal of Refrigeration*, Guildford, n.33, p.635-644, 2010.
- [11] Hesarakı, A.; Holmberg, S.; Haghighat, F. Seasonal thermal energy storage with heat pumps and low temperatures in building projects - A comparative review. *Renewable and Sustainable Energy Reviews*, Amsterdam, n. 43, p.1199-1213, 2015.
- [12] Ferrarez, A. H.; Oliveira Filho, D.; Teixeira, C. A. Independência Energética de Granja Suinícola a partir do uso de biogás. *Engenharia na Agricultura*, Viçosa, MG, v.18, n.3, p. 248-257, 2010.
- [13] Cervi, R. G.; Esperancini, M. S. T.; Bueno, C. Viabilidade econômica da utilização do biogás produzido em granja suinícola para geração de energia elétrica. *Engenharia Agrícola*, Jaboticabal, v.30, n.5, p.831-844, 2010.
- [14] Martins, F. M.; Oliveira, P. A. V. Análise econômica da geração de energia elétrica a partir do biogás na suinocultura. *Engenharia Agrícola*, Jaboticabal, v.31, n.3, p.477-486, 2011.
- [15] P. Neksa, "CO₂ heat pump systems," *Int. Journal of Refrigeration*, vol. 25, no. 4, pp. 421-427, June 2002.
- [16] M. H. Kim, J. Pettersen, and C. W. Bullard, "Fundamental process and system design issues in CO₂ vapor compression systems," *Progress in Energy and Combustion Science*, vol. 30, no. 2, pp. 119-174, 2004.
- [17] P. Neksa, H. Rekstad, G. R. Zakeri, and P. A. Schiefloe, "CO₂ heat pump water heater: characteristics, system design & experimental results," *Int. Journal of Refrigeration*, vol. 21, no. 3, pp. 172-179, May 1998.
- [18] S. D. White, M. G. Yarrall, D. J. Cleland, and R. A. Hedley, "Modelling the performance of a transcritical CO₂ heat pump for high temperature heating," *Int. Journal of Refrigeration*, vol. 25, no. 4, pp. 479-486, June 2002.
- [19] M. G. Yarral, S. D. White, D. J. Cleland, R. D. S. Kallu, and R. A. Hedley, "Performance of transcritical CO₂ heat pump for simultaneous refrigeration and water heating," *XX Int. Congress of Refrigeration*, Sydney, 1999, Paper no. 651.
- [20] W. Adriansyah, "Combined air conditioning and tap water heating plant using CO₂ as refrigerant," *Energy and Buildings*, vol. 36, no. 7, pp. 690- 695, July 2004.
- [21] J. Stene, "Residential CO₂ heat pump system for combined space heating and hot water heating," *Int. Journal of Refrigeration*, vol. 28, no. 8, pp. 1259-1265, Dec. 2005.
- [22] H. Cho, C. Ryu, Y. Kim, and H. Y. Kim, "Effects of refrigerant charge amount on the performance of a transcritical CO₂ heat pump," *Int. Journal of Refrigeration*, vol. 28, no. 8, pp. 1266-1273, Dec. 2005.
- [23] S. G. Kim, Y. J. Kim, G. Lee, and M. S. Kim, "The performance of a transcritical CO₂ cycle with an internal heat exchanger for hot water heating," *Int. Journal of Refrigeration*, vol. 28, no. 7, pp. 1064-1072, Nov. 2005.
- [24] J. Sarkar, S. Bhattacharyya, and M. Ramgopal, "Simulation of a transcritical CO₂ heat pump cycle for simultaneous cooling and heating applications," *Int. Journal of Refrigeration*, vol. 29, no. 5, pp. 735-743, Aug. 2006.
- [25] R. Yokoyama, T. Shimizu, K. Ito, and K. Takemura, "Influence of ambient temperatures on performance of a CO₂ heat pump water heating system," *Energy*, vol. 32, no. 4, pp. 388-398, Apr. 2007.

- [26] R. Cabello, D. Sa´nchez, R. Llopis, and E. Torrella, “Experimental evaluation of the energy efficiency of a CO₂ refrigerating plant working in transcritical conditions,” *Applied Thermal Engineering*, vol. 28, no. 13, pp. 1596-1604, Sep. 2008.
- [27] Keshuov, S.,Omarov, R.,Tokmoldayev, Kunelbayev, M.,Amirseit, S. Hybrid system for using renewable sources of energy for local consumers in agriculture. *Journal of Engineering and Applied Sciences* 12(5):1296-1306,2017
- [28] Rashit Omarov , Seitzkazy Keshuov , Dauren Omar , Asan Baibolov, Amanzhol Tokmoldayev and Murat Kunelbayev. Calculation of Heat Output of the Combined System with a Solar Collectors and Heat Pump. *Journal of Engineering and Applied Sciences* 12(6):1590-1598,2017